HHS Public Access

Author manuscript

Cancer Res. Author manuscript; available in PMC 2017 July 01.

Published in final edited form as:

Cancer Res. 2016 July 1; 76(13): 3884–3894. doi:10.1158/0008-5472.CAN-15-1524.

Renalase expression by melanoma and tumor associated-macrophages promotes tumor growth through a STAT3-mediated mechanism

Lindsay Hollander[1,4,6], **Xiaojia Guo**[1,4], **Heino Velazquez**[1,4,5], **John Chang**[1,5], **Robert Safirstein**[1,4,5], **Harriet Kluger**[3,4], **Charles Cha**[2,4,5], and **Gary V. Desir**[1,4,5]

[1]Department of Medicine

[2]Department of Surgery

[3]Department of Medical Oncology

[4]Yale School of Medicine

[5]Yale University, New Haven, CT, VACHS

[6]Department of Surgery, University of Connecticut, Farmington, CT

Abstract

To sustain their proliferation cancer cells overcome negative-acting signals that restrain their growth and promote senescence and cell death. Renalase (RNLS) is a secreted flavoprotein that functions as a survival factor after ischemic and toxic injury, signaling through the plasma calcium channel PMCA4b to activate the PI3K/AKT and MAPK pathways. We show that RNLS expression is increased markedly in primary melanomas and CD163+ tumor associated macrophages (TAM). In clinical specimens, RNLS expression in the tumor correlated inversely with disease-specific survival, suggesting a pathogenic role for RNLS. Attenuation of RNLS by RNAi, blocking antibodies or an RNLS-derived inhibitory peptide decreased melanoma cell survival, and anti-RNLS therapy blocked tumor growth in vivo in murine xenograft assays. Mechanistic investigations showed that increased apoptosis in tumor cells was temporally related to p38 MAPK-mediated Bax activation and that increased cell growth arrest was associated with elevated expression of the cell cycle inhibitor p21. Overall, our results established a role for the secreted flavoprotein RNLS in promoting melanoma cell growth and CD163+ TAM in the tumor microenvironment, with potential therapeutic implications for the management of melanoma.

INTRODUCTION

Renalase (RNLS), a novel secreted flavoprotein with oxidoreductase activity (1–5), functions as a survival factor and promotes cell and organ survival through a receptor-mediated process that is independent of its intrinsic enzymatic activities (6). Extracellular

Correspondence should be addressed to: Gary Desir, M.D., Section of Nephrology, Department of Medicine, Yale School of Medicine, P.O. Box 208029, New Haven, CT 06520-8029, Voice (203) 785-4119, gary.desir@yale.edu.

Conflicts of Interest: G Desir is a named inventor on several issued patents related to the discovery and therapeutic use of renalase. Renalase is licensed to Bessor Pharma, and G Desir holds an equity position in Bessor and its subsidiary Personal Therapeutics.

RNLS signals through the plasma membrane calcium ATPase PMCA4b and activates the PI3K and MAPK pathways (7). We have identified the critical region of the RNLS molecule that mediates its cytoprotective effects, and showed that a 20 amino acid RNLS peptide (RP-220, aa 220–239: CIRFVSIDNKKRNIESSEIG), which is conserved in all known isoforms but is devoid of any detectable oxidase activity, was as equally effective as RNLS protein at protecting HK-2 cells and mice against toxic and ischemic injury (6). Furthermore, RNLS and RP-220 rapidly activated protein kinase B (AKT), extracellular signal-regulated kinase (ERK), and the mitogen activated protein kinase (p38).

Since RNLS functions as a survival factor that engages the MAPK and PI3K pathways, and because its expression is regulated by STAT3 (8), we asked if RNLS expression and signaling provided a survival advantage to cancer cells. We focused on melanoma, a disorder in which the MAPK, PI3K and JAK/STAT pathways are regulated abnormally, and for which additional therapeutic targets would be desirable.

Skin cancer is a common human malignancy, and its incidence has been increasing in developed countries (9–11). Melanoma is the deadliest form of skin cancer, with low survival rates once it becomes unresectable (10). It is a molecularly heterogeneous disease and some of the key alterations in signaling pathways that participate in disease development and progression have been identified. The Ras/Raf/MEK/ERK and the PI3K/AKT signaling pathways play key roles in the pathogenesis of melanoma (9,11,12). Mutations in Ras, Raf, PI3K or PTEN (PI3K inhibitor) can lead to the sustained activation of ERK and AKT, which in turn promote cell survival and proliferation. Dankort et al. demonstrated this well with conditional melanocyte-specific expression of $BRaf^{V600E}$ in mice, none of whom developed melanoma, however, revealed 100% penetrance of melanoma development when combined with silencing of the *Pten* tumor suppressor gene (13). The elucidation of these pathogenic pathways has facilitated the development of specific inhibitors that target hyper-activated kinases. While these agents have proven effective in the treatment of selective groups of patients with metastatic melanoma, their beneficial actions are often short lived, hence the pressing need for the identification of additional therapeutic targets.

MATERIAL AND METHODS

Reagents

Human melanoma cell lines A375.S2, SkMel28, SkMel5, MeWo, and WM266-4 were obtained from the American Type Culture Collection and maintained as recommended. Mouse metastatic melanoma cell line B16f10 was obtained from American Type Culture Collection. Cells were used within six months of purchase, and a link to the method of authentication is provided here: http://www.atcc.org/support/faqs/eae27/Authenticating%20cell%20lines-249.aspx.

Recombinant human RNLS was expressed, purified, concentrated, and dialyzed against PBS as described (14). RNLS peptides RP220 and mutated peptide RP220A were synthesized at United Peptide. Rabbit anti-RNLS monoclonal antibody (ab178700), goat polyclonal anti-RNLS antibody (ab31291), goat IgG and rabbit IgG were purchased from Abcam. Anti-

RNLS monoclonal antibodies m28-RNLS and m37-RNLS were synthesized as previously described (15).

Tissue specimens

Human melanoma cDNA arrays I and II were obtained from OriGene Technologies (Rockville, MD, USA). The relevant pathology reports are available online: http://www.origene.com/assets/documents/TissueScan. Human melanoma and normal skin tissue samples obtained from US Biomax (Rockville, MD, USA) were used for immunohistochemistry or immunofluorescence. The relative expression levels of various genes were assessed by quantitative (q)RT-PCR, as described previously (15)

Immunohistochemical staining and western blot analysis

Immunohistochemistry was performed as described previously (16). A detailed desccription is available in the Supplement. Western blot analysis was carried out as previously described (6).

Tissue microarray

Melanoma tissue microarrays were purchased from US BioMax, Inc. and Yale tissue pathology services. This study was approved by the Human Investigation Committee of Yale University School of Medicine (HIC protocol No. 1003006479). The Yale melanoma tissue microarray was constructed as previously described (17,18). A total of 570 tissue cores representing 542 total melanoma cases and a small series of controls measuring 0.6 mm were spaced 0.8 mm apart on a single glass slide. The cohort was constructed from formalin-fixed, paraffin-embedded tissue blocks obtained from the archives of the Department of Pathology at Yale University School of Medicine. A pathologist examined each case to select the region for inclusion in the tissue microarray. Core biopsies from the specimens were placed on the tissue microarray with a Tissue Micorarrayer (Beecher Instruments, Sun Prairie, WI). The tissue microarrays were then cut to 5-um sections and placed on glass slides with the adhesive tape transfer system (Instumedics, Inc., Hackensack, NJ) with UV cross-linking. The specimens were all drawn from archives of tumors resected between 1959 and 1994, with a follow-up range of 2 months and 38 years (median follow-up time, 60 months). The cohort characteristics are described previously (19).

The tissue microarray slide was stained as described previously (19,20). A detailed desccription is available in the Supplement.

Cell Viability Assays

Total cell number and percentage of live cells were assessed by trypan blue exclusion, and cells were counted using a BioRad TC10 automated cell counter. For additional studies, cell viability was determined using WST-1 reagent (Roche Diagnostics, Indianapolis, IN, USA) as previously described (6).

RNA interference

Four individual siRNAs and a siRNA SMART pool targeting RNLS were purchased from Dharmacon (Lafayette, CO, USA). Cells were transfected with RNLS siRNA or a universal

negative control small interfering RNA (control siRNA, Dharmacon) using DharmaFECT 4 reagent (Dharmacon) as instructed by the manufacturer. Knock-down efficiency was determined by qPCR.

Mouse tumor model

Female athymic, 18–20 g nude mice (nu/nu) were obtained from Charles River (Willimantic, CT) and housed in microisolator cages, with autoclaved bedding in a specific pathogen-free facility, with a 12-h light/dark cycle. Animals received water and food ad libitum, and were observed for signs of tumor growth, activity, feeding and pain, in accordance with the study protocol approved by the VACHS IACUC.

Xenograft tumors were established by subcutaneous injection of A375.S2 cells (2×10^6 in 100 μl of PBS, pH 7.6). When the tumors reached a volume of 50–100 mm^3, the mice were divided into a control group (n=14 treated with rabbit IgG, 40 μg by intraperitoneal injection (IP) once weekly, and 40 ug subcutaneously (SQ) around the tumor site every 3 days), and an experimental group (n=14) that received m28-RNLS (40 μg IP, once weekly, and 40 ug SQ, every 3 days). Tumor size was measured with digital calipers and volume was calculated according to the formula (length × $width^2$) x $\pi/2$. Apoptosis was quantified using the TUNEL assay as previously described (15).

Isolation and polarization of bone marrow-derived macrophages

Femur and tibial bones were isolated from 10-week old male C57BL/6 (Harlan Spraugue Dawley) or RNLS-/- mice (21) and bone marrow cells were pelleted and resuspended in Macrophage-SFM (Gibco, Cat# 12065-074) supplemented with 5ng/ml mouse recombinant macrophage-colony stimulating factor (mM-CSF, ConnStem, Inc., Cat# M2000) at 2×10^6 macrophages/ml. Adherent macrophages were incubated in Macrophage-SFM plus mM-CSF at 30 ng/ml for additional 4 days. On Day 5 post isolation, fresh medium containing either 50ng/ml interleukin 6 (IL-6, R&D System, Cat#406-ML) or 50ng/ml leukemia inhibitory factor (LIF, R&D System, Cat#8878-LF) was added to polarize macrophage to M2d TAM. IL-10 measurements were obtained by qPCR 48 hours later.

Statistical analysis of the data was carried out as previously described (15). A detailed desccription is available in the Supplement.

RESULTS

RNLS overexpression in melanoma

In order to determine if RNLS expression differed between normal human skin and malignant melanoma, we examined tissue microarrays (TMAs; Yale Tissue Microarray Facility and US Biomax, Inc.) spanning the progression of normal skin to benign nevus to primary and metastatic melanoma. The Yale TMAs contained formalin-fixed, paraffin-embedded specimens obtained from a cohort of 192 primary melanomas collected during 1959 to 1994, a cohort of 246 serial primary and metastatic melanomas collected from 1997 to 2004, a cohort of 295 patients with benign nevi, and matched normal skin specimens from 15 patients. The demographics and clinical characteristics for these tissue microarrays have

been described previously (22). The US Biomax array contained 74 specimens, including 35 primary melanomas, 11 metastatic lesions, 14 benign nevi, and 14 normal samples. Examination of approximately 600 histospots for RNLS protein expression using a quantitative, automated immunofluorescence (IF) microscopy system (AQUA), revealed that progression from normal skin to benign nevi to primary malignant melanoma to metastatic melanoma was accompanied by a significant increase in RNLS expression ($p=0.009$, $p=0.0003$, and $p<0.001$, respectively, Figure 1a–c).

We asked if dysregulated RNLS expression and signaling could facilitate melanoma growth, and, therefore, serve as a prognostic marker. We examined each primary melanoma from a cohort of 246 serial primary and metastatic samples collected from 1997 to 2004. One hundred nineteen patients had histospots that were suitable for evaluation by AQUA technology. In this group, we compared the outcome of patients whose tumors expressed high RNLS levels (RNLS AQUA score > median AQUA score 75,764.45) to those with low RNLS expression. High RNLS expression was associated with increased melanoma-specific death: 5- year and 10-year disease-specific survival rates of 55% versus 69% and 39.7% versus 58.5%, respectively, $p=0.008$, (Figure 1d). Following multivariate analysis of this cohort, RNLS levels were found to be independently predictive of survival in melanoma ($p=0.004$, HR=3.130). Stage of disease at diagnosis ($p=0.05$, HR=3.940), Clark level ($p=0.015$, HR=1.687), and ulceration of the primary tumor ($p=0.001$, HR=2.54) were also found to independently predict survival in melanoma. The 5-year survival rate for patients with tumors containing lower levels of infiltrating CD163+ macrophage (M2 like phenotype, tumor promoting) was 52% compared to 42% ($p<0.04$) for those with tumors with higher levels of CD163+ cells. These findings suggest that RNLS expression may serve as a useful prognostic marker in melanoma, and may help identify a subset of patients with a more aggressive phenotype.

RNLS overexpression favors cancer cell survival

RNLS-mediated signaling is anti-apoptotic, and protects normal cells exposed to toxic stress from apoptotic death (23,24). To explore if RNLS signaling favored the survival of cancer cells, either recombinant RNLS (rRNLS) or bovine serum albumin (BSA) was added to serum-starved melanoma cells (A375.S2, MeWo, SkMel5, and SkMel28) in culture, and cell viability was determined. Compared to BSA, RNLS markedly increased the survival of serum-starved cells, and caused an apparent increase in the proliferative rate as measured by the WST-1 assay ($n=6$, $p<0.05$, Figure 2a). The total cell number and percentage of live cells of those treated with RNLS were counted to determine if the apparent increase in proliferative rate was due an increase in cell proliferation or to a decrease in the rate of apoptosis. As shown in Figure 2b, treatment with RNLS showed increased cell counts, and increased percentage of live cells compared to those treated with BSA, suggesting that RNLS functions as an anti-apoptotic, survival factor.

Inhibition of RNLS signaling is cytotoxic to melanoma cells in vitro

We used 3 approaches to determine the functional consequences of inhibiting RNLS expression and signaling in melanoma. First, we evaluated the effect of decreasing RNLS expression on cell viability. RNLS knockdown by siRNA markedly reduced the viability of

the melanoma cell lines A375.S2 and SkMel28 (p=0.03 and p=0.003, respectively, Figure 3a). Second, since the RNLS peptide RP-220 mimics the protective effect and signaling properties of rRNLS, we reasoned that it likely interacts with a critical region of the receptor for extracellular RNLS and that antibodies directed against it could have inhibitory properties. Therefore, we developed a panel of monoclonal antibodies against RP-220, and tested their effect on cancer cell survival. Two monoclonal antibodies generated against RNLS, [clones # 28-4 (m28-RNLS), 37-10 (m37-RNLS)] decreased the viability of all (total of 5) melanoma cell lines tested, and representative examples are shown in Figures 3b–c. m28-RNLS demonstrated increasing levels of cytotoxicity in correlation with increasing treatment concentrations ($p<0.05$, Figure 3b). Third, we generated a peptide antagonist (RP-220A) by decreasing RP-220's net charge (3 Lysine/arginine changed to alanine Figure 3d). RP220A does not mediate RNLS dependent signaling, but binds to PMCA4b and antagonizes the action of endogenous RNLS (7). RP-220A proved to be cytotoxic in increasing doses to melanoma cells in culture ($p<0.005$, Figure 3d).

Inhibition of RNLS signaling blocks tumor growth in vivo

We injected A375.S2 (human melanoma) cells subcutaneously into athymic nude mice to generate tumors. Once the tumors reached a volume of ~50 mm^3, the animals were then treated with either control rabbit IgG or a RNLS neutralizing monoclonal antibody, m28-RNLS. As overall animal health and activity was maintained throughout the study, the antibody treatment did not appear to be toxic. Tumor size was measured every other day, and treatment with m28-RNLS decreased tumor volume at all points tested ($p<0.05$, Figure 4a). The animals were sacrificed at day 11 due to overall tumor size and ulceration in some animals. IHC staining of sections from the xenografted tumors with the cellular proliferation marker Ki67 revealed a significant decrease in cellular proliferation within the tumors treated with the anti-RNLS antibody versus to those treated with rabbit IgG: of 35.1±2.3 positive cells/high power field in the control group vs. 13.4±3.0 in the RNLS Ab treated group, n=14, p=0.0004 (Figure 4b). To test the efficacy of anti-RNLS therapy in immunocompetent, B16f10 cells (mouse melanoma line) were subcutaneously into C57BL/6 mice. Once the tumors reached a volume of ~500mm^3, the animals were treated with either control rabbit IgG or a RNLS neutralizing monoclonal antibody, m28-RNLS and sacrificed at day 7 due to the very large tumor burden of the control group. As depicted in figure 4c, m28-RNLS administration caused a significant reduction in tumor volume compared to rabbit IgG.

Inhibition of RNLS signaling blocks endogenous RNLS expression and STAT3 activation and induces apoptosis and cell cycle arrest

STAT3 is known to bind to the promoter region of the RNLS gene and increase its expression, and a positive RNLS-STAT3 feedback loop has been suggested (8). This relationship was further investigated through immunofluorescent tissue staining and study of the cell lysates from the xenografted tumors treated with control IgG and m28-RNLS. Significant coexpression of RNLS with phosphorylated and total STAT3 was noted in the tumor samples (Figure 5a) as assessed by IF. Treatment with m28-RNLS caused a dramatic reduction in RNLS protein expression, and in both total and phosphorylated STAT3 (Figure 5a). Changes in protein expression were confirmed by western blot as shown in Figure 5b–c.

In tumors treated with m28-RNLS, STAT3 phosphorylation at tyrosine 705 (p-Y^{705}-STAT3), and total STAT3 were significantly decreased (n=8, p<0.005, Figure 5b–c).

To test if the significant decrease in RNLS expression was primarily occurring in the melanoma cells, we used human and mouse specific primers to amplify tumor (human) and endogenous (mouse) RNLS in the tumor mass. As depicted in Figure 5d, treatment with m28-RNLS causes a significant reduction in mouse RNLS expression, without affecting human (tumor) expression, suggesting that tumor-infiltrating cells play a key role in RNLS production and secretion.

In addition, we noted increased expression of the cell cycle inhibitor p21. Antibody treatment markedly increased the expression of the cell cycle regulator p21 in the tumor samples: 24.2±2.4 positive cells in the antibody treated group vs. 12.2±1.0 in the control group, n=14, p=0.009 (Figure 5e). Terminal deoxynucleotidyl transferase dUTP nick end labeling (TUNEL) staining revealed a significant increase in the average number of cells undergoing apoptosis in the antibody-treated tumors over the control group with an average of 13.3±0.6 positive cells vs. 4.3±0.2, n=14, p<0.001, (Figure 5e). The increase in apoptosis was temporally related to phopshorylation of p38 MAPK, and subsequent activation of the B-cell lymphoma 2 related protein Bax (Figure 5f). These data indicate that treatment with anti-RNLS antibody causes a marked reduction in total and phosphorylated STAT3, decreases cell proliferation, and increases apoptosis in tumor cells.

Plasma membrane Ca ATPase PMCA4b mediates RNLS dependent STAT3 and ERK1/2 phosphorylation in B16-F10 melanoma cells

We've previously identified PMCA4b as a receptor for extracellular RNLS (7). PMCA4b is overexpressed in colon and breast cancer, and its catalytic domain interacts with the proapoptotic tumor suppressor Ras-associated factor 1 (RASSF1) to inhibit EGF dependent ERK phosphorylation (25–27). PMCA4b expression in human melanoma cell lines was confirmed by western blotting, and qPCR (Figures 6a–b). To study the interaction of PMCA4b and RNLS in melanoma, we tested for co-expression of both proteins in B16-F10 xenografts. Data obtained from control animals (Figure 6c, **top panel**) indicate high expression of PMCA1/4, along with significant coexpression with RNLS. In animals treated with m28-RNLS, the expression of both proteins is diminished, as is the extent of coexpression (Figure 6c bottom panel). B16-F10 cells grown in serum free medium express and secrete RNLS (Figure 6d).

To examine PMCA4b's role in RNLS-dependent signaling in B16-F10 cells, we decreased its expression using siRNA and compared RNLS mediated ERK and STAT3 signaling. In control studies, non-targeting siRNAs affected neither PMCA4b gene expression (assessed by qPCR), nor RNLS-mediated ERK or STAT3 phosphorylation as evidenced by the expected transient activation most notable at the 5 min time point (Figure 6e, left panel). In contrast, PMCA4b-targeting siRNAs decreased gene expression by 85±4% (n=3), and reduced RNLS dependent ERK and STAT3 phosphorylation by ~ 90% (Figure 6e, right panel).

To examine PMCA4b's role in RNLS-mediated signaling in macrophages, we used siRNA to decrease its expression in Raw 264.7, a macrophage cell line derived from mouse blood. In control studies, non-targeting siRNAs affected neither PMCA4b gene expression (assessed by qPCR), nor RNLS-mediated ERK phosphorylation. As shown in Figure 6f (left panel), the expected transient ERK activation by RNLS most notable at the 10 min time point. PMCA4b-targeting siRNAs decreased gene expression by 79±2% (n=4), and reduced RNLS dependent ERK1/2 phosphorylation by ~ 95% (Figure 6f, right panel).

In contrast to what's observed in B16F10 (Figure 6e), Panc1 pancreatic cancer cells (15), and the human kidney cell HK-2 (28), RNLS does not activate STAT3 in Raw 264.7 macrophage cells (Figure 6f). To test if RNLS signaled via STAT3 in non-transformed macrophages, we treated bone marrow derived (BMDM) non-polarized macrophages (MØ) with rRNLS. As shown in Figure 6G, RNLS-mediated STAT3 phosphorylation was not detected in BMDM, MØ suggesting that in contrast to other cells, RNLS does not activate the STAT3 pathway in macrophages.

Inhibition of RNLS signaling increases the ratio of CD86^{+} to CD163+ TAMs

The melanocytes did not appear to be the main source of the RNLS in the melanoma histospots, as there was minimal overlap noted between RNLS and melanocyte staining (Figure 1a). Melanomas often have significant infiltration of immune cells, including macrophages. The infiltrating macrophages appeared to contribute the majority of the tumoral RNLS as a substantial component of the RNLS staining noted in each histospot overlapped significantly with the pan-macrophage marker CD68 (Figure 7a top panel). Upon further investigation, we determined that RNLS was coexpressed predominantly with CD163+ (M2-like) TAMs (Figure 7a, middle panel). Coexpression of RNLS with CD86+ (M1-like) macrophages was minimal (Figure 7a, bottom panel). M2-like (CD163+) macrophages are associated with immune escape and shown to promote cancer development and spread, while M1-like (CD86+) macrophages are typically pro-inflammatory, and inhibit tumor growth (29,30).

We have examined RNLS expression in macrophages infiltrating tumor xenografts in nude mice. Figure 7b is a representative picture of RNLS expression in CD68+ cells (pan macrophage marker) in the tumor mass (n=4) of control animals treated with rabbit IgG. Manual count of cells expressing RNLS, CD68 or both indicates that 60% of cells expressing RNLS also express CD68, and that 25% of CD68+ cells express RNLS. Treatment of the xenografts with m28-RNLS antibody led to a marked decrease in the number of CD163+ TMAs, and the remaining cells did not express detectable levels of RNLS (Figure 7c).

Although catecholamines and nicotine have been shown to upregulate RNLS gene expression in epithelial cells (8,31), we have no knowledge of the signals that affect RNLS expression in macrophages. We hypothesized that tumor cells could modulate RNLS expression by macrophage, and that RNLS could facilitate macrophage polarization toward a M2d like, tumor promoting phenotype. This was tested by examining the effect of conditioned media (CM) obtained from cultured murine melanoma cells (B16f10) on RNLS expression by bone marrow derived, non-polarized macrophages (MØ). As shown in figure

7d, the addition of B16f10 CM stimulated an 8 fold increase RNLS expression in MØ compared to control, indicating that factor(s) secreted by melanoma markedly upregulate RNLS in macrophages. As shown in Figure 6f, our data suggest that RNLS activates ERK1/2, but not STAT3, in an autocrine fashion in MØ. In order to examine the potential phenotypic consequence of RNLS expression in MØ, we compared the response of WT and RNLS deficient MØ to 2 stimuli [IL-6 and Leukemia inhibitory factor (LIF)] reported to polarize MØ toward a tumor promoting M2d phenotype (32). We find that IL-6 and LIF stimulated IL-10 gene expression significantly more in WT than in KO macrophages (Figure 7e).

DISCUSSION

RNLS expression is markedly increased in melanoma cell lines and tumor samples. In patients with metastatic melanoma, RNLS expression is inversely correlated with disease-specific survival. Examination of the pattern of expression of RNLS in melanoma suggests that up-regulation predominantly occurs in the cellular components of tumor-associated stroma, specifically in CD163+ macrophages. Experimental data indicate that alternatively activated macrophages (M2-like, $CD163^+$) recruited into the tumors suppress the immune response against the tumor, increase angiogenesis, and facilitate tumor cell migration, invasion and dissemination (33–35). TAMs account for a significant percentage of the tumor mass in human melanoma, and also in the xenograft model described in this work. We find that RNLS is preferentially expressed in $CD163^+$ TAMs, suggesting that M2-like TAMs could facilitate tumor progression by secreting RNLS, which in turn would act in a paracrine fashion to promote tumor growth. Figure 7f illustrates a working model that incorporates the key mechanisms that underlie the anti-tumor effects observed with inhibition of RNLS signaling. Inhibition of RNLS signaling by the RNLS monoclonal m28-RNLS increases the ratio of $CD86^+$ to $CD163^+$ TAMs, and decreases RNLS secretion by $CD163^+$ TAMs. RNLS is expressed in other cells and tissues and circulates in plasma. m28-RNLS has a direct effect on melanoma cells by inhibiting RNLS signaling. The net result is a dramatic fall in total and phosphorylated STAT3, leading to apoptosis of melanoma cells.

The regulatory promoter elements and transcription factors that regulate RNLS gene expression have been recently investigated (8) and these data point to a key role for STAT3. Our results suggest the existence of a feedforward loop between RNLS and STAT3, in which signals that upregulate STAT3 increase RNLS gene expression, which in turn increases STAT3 activity. The existence of such an interaction between RNLS and STAT3 has important implications regarding the role of RNLS signaling in the pathogenesis of cancer. Indeed, there are extensive data pointing to a key role for the STAT family proteins, particularly STAT3, in the induction and maintenance of an inflammatory microenvironment that facilitates malignant transformation and cancer progression (36). STAT3 signaling is often persistently activated in malignant cells, and such activation not only drives tumor cell proliferation, but also increases the production of a large number of genes that sustain inflammation in the tumor microenvironment. A STAT3 feed-forward loop between cancer cells and non-transformed and stromal cells has been documented in cancer (37–39). For instance, STAT3 is constitutively activated in multiple myeloma patients. In the IL-6-dependent human myeloma cell line U266, IL-6 signals through Janus kinases to activate

STAT3, which in turn up-regulates anti-apoptotic factors, and promotes the survival of tumor cells (37). Through various mechanisms, STAT3 has also been found to be constitutively activated in a majority of melanomas leading to increases in tumor cell survival, proliferation, metastasis, angiogenesis, and decreases in tumor immune response(11,40–42).

RNLS protects against ischemic renal and cardiac injury (21,43,44). The promoter region of the RNLS gene contains four potential hypoxia-inducible factor-1 alpha (HIF-1α) response elements, and has been shown to represent novel target gene of HIF-1α (44). These data raise the intriguing possibility that certain physiological and pathophysiological effects of HIF-1α in normal cells may be mediated by RNLS, and this could also be relevant to cancer pathogenesis, and progression.

RNLS mediates cytoprotection by increasing the anti-apoptotic factor Bcl2, and preventing the activation of effector caspases (6). Since RNLS is an NADH oxidase (1), it is possible that its protective action is in part mediated by its enzymatic properties (21,24,45). Inhibition of RNLS signaling in A375.S2 cells is associated with sustained activation of p38 MAPK, followed by activation of the apoptotic factor Bax, and apoptosis. The MAPK p38 is a stress-activated protein kinase that has been implicated in inflammation, cell differentiation, cell cycle regulation and apoptosis (46). For instance, nerve growth factor withdrawal was shown to cause apoptosis following sustained activation of JNK and p38, and down-regulation of ERK (47). However, since under certain conditions inhibition of p38 can block apoptosis (46), p38's role in apoptosis is clearly context dependent. Our data suggest that in A375.S2 cells, RNLS dependent activation of p38 causes apoptosis.

Inhibition of RNLS signaling markedly decreases the expression of Ki-67 in xenographs of melanoma, and we interpret the data as indicating that RNLS signaling is a key driver of tumor proliferation, and that RNLS inhibition decreases the proliferative rate of tumors. Many of the key factors that determine cell cycle progression have been identified, and include a set of cyclin dependent kinases (CDKs) along with two classes of CDK inhibitors (48). The expression of p21, a CDK inhibitor belonging to the CIP/KIP family, is regulated by RNLS signaling. Inhibition of RNLS signaling is associated with a marked increase in p21 expression. p21 is a negative regulator of cell cycle that can maintain cells in G0, block G1/S transition, and cause G1 or inter-S phase arrest (48). Therefore, the increase in p21 expression could account for the decrease in cell proliferation observed in tumors treated with an anti RNLS antibody. In addition, p38 has also been shown to affect cell cycle progression (46), and activation of p38 by anti RNLS treatment could also contribute to cell cycle arrest.

Our findings identify RNLS as a secreted protein that can promote the survival and growth of cancer cells, and provide a framework to further investigate the use of anti RNLS therapy for the treatment of malignant melanoma, alone or in conjunction with other TAM- or melanoma-inhibiting drugs, such as CSF-1R inhibitors or MAPK pathway inhibitors, respectively. Because there are multiple mechanisms for regulating MAPK and PI3K and JAK/STAT3 and since there is crosstalk between pathways, cell fate depends on the dynamic balance and integration of multiple signals, and our data suggest that RNLS inhibition will tilt the balance toward cancer cell death.

Supplementary Material

Refer to Web version on PubMed Central for supplementary material.

Acknowledgments

Funding Sources

This work was supported in part by VA Connecticut (H. Velazquez, R. Safirstein. and G.V. Desir), National Institute of Health grants RC1DK086465, RC1DK086402 and R01DK081037 (G.V. Desir), National Cancer Institute Research Grant CA-16359, and the Lampman surgical award from Yale University Department of Surgery (C. Cha).

We thank Dr Ruth Halaban for helpful comments and suggestions.

Literature Cited

1. Farzaneh-Far R, Desir GV, Na B, Schiller NB, Whooley MA. A functional polymorphism in renalase (Glu37Asp) is associated with cardiac hypertrophy, dysfunction, and ischemia: data from the heart and soul study. PLoS One. 2010; 5(10):e13496. [PubMed: 20975995]
2. Desir GV, Tang L, Wang P, Li G, Sampaio Maia B, Quelhas-Santos J, et al. Renalase lowers ambulatory blood pressure by metabolizing circulating catecholamines. J Am Heart Assoc. 2012; 1:e002634. [PubMed: 23130169]
3. Desir GV, Wang L, Peixoto AJ. Human renalase: a review of its biology, function, and implications for hypertension. Journal of the American Society of Hypertension. 2012
4. Xu J, Li G, Wang P, Velazquez H, Yao X, Li Y, et al. Renalase is a novel, soluble monoamine oxidase that regulates cardiac function and blood pressure. J Clin Invest. 2005; 115(5):1275–80. [PubMed: 15841207]
5. Li G, Xu J, Wang P, Velazquez H, Li Y, Wu Y, et al. Catecholamines regulate the activity, secretion, and synthesis of renalase. Circulation. 2008; 117(10):1277–82. [PubMed: 18299506]
6. Wang L, Velazquez H, Moeckel G, Chang J, Ham A, Lee HT, et al. Renalase Prevents AKI Independent of Amine Oxidase Activity. Journal of the American Society of Nephrology. 2014; doi: 10.1681/asn.2013060665
7. Wang L, Velazquez H, Chang J, Safirstein R, Desir GV. Identification of a Receptor for Extracellular Renalase. PLoS ONE. 2015; 10(4):e0122932. [PubMed: 25906147]
8. Sonawane PJ, Gupta V, Sasi BK, Kalyani A, Natarajan B, Khan AA, et al. Transcriptional Regulation of the Novel Monoamine Oxidase Renalase: Crucial Roles of Transcription Factors Sp1, STAT3 and ZBP89. Biochemistry. 2014
9. Gray-Schopfer V, Wellbrock C, Marais R. Melanoma biology and new targeted therapy. Nature. 2007; 445(7130):851–57. [PubMed: 17314971]
10. Lowe GC, Saavedra A, Reed KB, Velazquez AI, Dronca RS, Markovic SN, et al. Increasing Incidence of Melanoma Among Middle-Aged Adults: An Epidemiologic Study in Olmsted County, Minnesota. Mayo Clinic Proceedings. 2014; 89(1):52–59. [PubMed: 24388022]
11. Lesinski GB. The potential for targeting the STAT3 pathway as a novel therapy for melanoma. Future oncology. 2013; 9(7):925–7. [PubMed: 23837753]
12. Yajima I, Kumasaka MY, Thang ND, Goto Y, Takeda K, Yamanoshita O, et al. RAS/RAF/MEK/ERK and PI3K/PTEN/AKT Signaling in Malignant Melanoma Progression and Therapy. Dermatology research and practice. 2012; 2012:354191. [PubMed: 22013435]
13. Dankort D, Curley DP, Cartlidge RA, Nelson B, Karnezis AN, Damsky WE Jr, et al. Braf(V600E) cooperates with Pten loss to induce metastatic melanoma. Nature genetics. 2009; 41(5):544–52. [PubMed: 19282848]
14. Desir GV, Tang L, Wang P, Li G, Sampaio-Maia B, Quelhas-Santos J, et al. Renalase lowers ambulatory blood pressure by metabolizing circulating adrenaline. Journal of the American Heart Association. 2012; 1(4):e002634. [PubMed: 23130169]

15. Guo X, Hollander L, MacPherson D, Wang L, Velazquez H, Chang J, et al. Inhibition of renalase expression and signaling has antitumor activity in pancreatic cancer. Scientific Reports. 2016; 6:22996. [PubMed: 26972355]
16. Guo X, Schmitz JC, Kenney BC, Uchio EM, Kulkarni S, Cha CH. Intermedin is overexpressed in hepatocellular carcinoma and regulates cell proliferation and survival. Cancer science. 2012; 103(8):1474–80. [PubMed: 22625651]
17. Berger AJ, Kluger HM, Li N, Kielhorn E, Halaban R, Ronai Z, et al. Subcellular localization of activating transcription factor 2 in melanoma specimens predicts patient survival. Cancer research. 2003; 63(23):8103–7. [PubMed: 14678960]
18. Rimm DL, Camp RL, Charette LA, Costa J, Olsen DA, Reiss M. Tissue microarray: a new technology for amplification of tissue resources. Cancer journal. 2001; 7(1):24–31.
19. Berger AJ, Camp RL, Divito KA, Kluger HM, Halaban R, Rimm DL. Automated quantitative analysis of HDM2 expression in malignant melanoma shows association with early-stage disease and improved outcome. Cancer Res. 2004; 64(23):8767–72. [PubMed: 15574789]
20. Nicholson AD, Guo X, Sullivan CA, Cha CH. Automated quantitative analysis of tissue microarray of 443 patients with colorectal adenocarcinoma: low expression of Bcl-2 predicts poor survival. Journal of the American College of Surgeons. 2014; 219(5):977–87. [PubMed: 25127509]
21. Wu Y, Xu J, Velazquez H, Wang P, Li G, Liu D, et al. Renalase deficiency aggravates ischemic myocardial damage. Kidney Int. 2011; 79(8):853–60. [PubMed: 21178975]
22. Gould Rothberg BE, Berger AJ, Molinaro AM, Subtil A, Krauthammer MO, Camp RL, et al. Melanoma prognostic model using tissue microarrays and genetic algorithms. Journal of clinical oncology : official journal of the American Society of Clinical Oncology. 2009; 27(34):5772–80. [PubMed: 19884546]
23. Wang L, Velazquez H, Moeckel G, Chang J, Ham A, Lee HT, et al. Renalase Prevents AKI Independent of Amine Oxidase Activity. J Am Soc Nephrol. 2014
24. Lee HT, Kim JY, Kim M, Wang P, Tang L, Baroni S, et al. Renalase protects against ischemic AKI. J Am Soc Nephrol. 2013; 24(3):445–55. [PubMed: 23393318]
25. Armesilla AL, Williams JC, Buch MH, Pickard A, Emerson M, Cartwright EJ, et al. Novel Functional Interaction between the Plasma Membrane Ca2+ Pump 4b and the Proapoptotic Tumor Suppressor Ras-associated Factor 1 (RASSF1). Journal of Biological Chemistry. 2004; 279(30): 31318–28. [PubMed: 15145946]
26. Agathanggelou A, Cooper WN, Latif F. Role of the Ras-Association Domain Family 1 Tumor Suppressor Gene in Human Cancers. Cancer Research. 2005; 65(9):3497–508. [PubMed: 15867337]
27. Brini M, Calì T, Ottolini D, Carafoli E. The plasma membrane calcium pump in health and disease. FEBS Journal. 2013; 280(21):5385–97. [PubMed: 23413890]
28. Guo X, Hollander L, MacPherson D, Wang L, Velazquez H, Chang J, et al. Inhibition of renalase expression and signaling has antitumor activity in pancreatic cancer. Scientifc Reports. 2016 In Press.
29. Biswas SK, Mantovani A. Macrophage plasticity and interaction with lymphocyte subsets: cancer as a paradigm. Nat Immunol. 2010; 11(10):889–96. [PubMed: 20856220]
30. Mantovani A, Sozzani S, Locati M, Allavena P, Sica A. Macrophage polarization: tumor-associated macrophages as a paradigm for polarized M2 mononuclear phagocytes. Trends in Immunology. 23(11):549–55. [PubMed: 12401408]
31. Xu J, Li G, Wang P, Velazquez H, Li Y, Wu Y, et al. Catecholamines regulate the activity, secretion and synthesis of renalase. Submitted for Publication 2007.
32. Duluc D, Delneste Y, Tan F, Moles M-P, Grimaud L, Lenoir J, et al. Tumor-associated leukemia inhibitory factor and IL-6 skew monocyte differentiation into tumor-associated macrophage-like cells. Blood. 2007; 110(13):4319–30. [PubMed: 17848619]
33. Ruhrberg C, De Palma M. A double agent in cancer: Deciphering macrophage roles in human tumors. Nat Med. 2010; 16(8):861–62. [PubMed: 20689550]
34. Pollard JW. Tumour-educated macrophages promote tumour progression and metastasis. Nat Rev Cancer. 2004; 4(1):71–78. [PubMed: 14708027]

35. Hao N-B, Lü M-H, Fan Y-H, Cao Y-L, Zhang Z-R, Yang S-M. Macrophages in Tumor Microenvironments and the Progression of Tumors. Clinical and Developmental Immunology. 2012; 2012:11.

36. Yu H, Pardoll D, Jove R. STATs in cancer inflammation and immunity: a leading role for STAT3. Nat Rev Cancer. 2009; 9(11):798–809. [PubMed: 19851315]

37. Catlett-Falcone R, Landowski TH, Oshiro MM, Turkson J, Levitzki A, Savino R, et al. Constitutive activation of Stat3 signaling confers resistance to apoptosis in human U266 myeloma cells. Immunity. 1999; 10(1):105–15. [PubMed: 10023775]

38. Yu H, Kortylewski M, Pardoll D. Crosstalk between cancer and immune cells: role of STAT3 in the tumour microenvironment. Nat Rev Immunol. 2007; 7(1):41–51. [PubMed: 17186030]

39. Ara T, Song L, Shimada H, Keshelava N, Russell HV, Metelitsa LS, et al. Interleukin-6 in the bone marrow microenvironment promotes the growth and survival of neuroblastoma cells. Cancer Res. 2009; 69(1):329–37. [PubMed: 19118018]

40. Kortylewski M, Jove R, Yu H. Targeting STAT3 affects melanoma on multiple fronts. Cancer metastasis reviews. 2005; 24(2):315–27. [PubMed: 15986140]

41. Emeagi PU, Maenhout S, Dang N, Heirman C, Thielemans K, Breckpot K. Downregulation of Stat3 in melanoma: reprogramming the immune microenvironment as an anticancer therapeutic strategy. Gene therapy. 2013; 20(11):1085–92. [PubMed: 23804077]

42. Yang CH, Fan M, Slominski AT, Yue J, Pfeffer LM. The role of constitutively activated STAT3 in B16 melanoma cells. International journal of interferon, cytokine and mediator research : IJIM. 2010; 2010(2):1–7.

43. Guo X, Wang L, Velazquez H, Safirstein R, Desir GV. Renalase: its role as a cytokine, and an update on its association with type 1 diabetes and ischemic stroke. Curr Opin Nephrol Hypertens. 2014; 23(5):513–8. [PubMed: 24992568]

44. Du M, Huang K, Huang D, Yang L, Gao L, Wang X, et al. Renalase is a novel target gene of hypoxia-inducible factor-1 in protection against cardiac ischaemia–reperfusion injury. Cardiovascular Research. 2014; 105(2):182–91. [PubMed: 25497549]

45. Wang L, Velazquez H, Moeckel G, Chang J, Ham A, Lee HT, et al. Renalase Prevents AKI Independent of Amine Oxidase Activity. Journal of the American Society of Nephrology. 2014; 25(6):1226–35. [PubMed: 24511138]

46. Ono K, Han J. The p38 signal transduction pathway Activation and function. Cellular Signalling. 2000; 12(1):1–13. [PubMed: 10676842]

47. Xia Z, Dickens M, Raingeaud J, Davis RJ, Greenberg ME. Opposing Effects of ERK and JNK-p38 MAP Kinases on Apoptosis. Science. 1995; 270(5240):1326–31. [PubMed: 7481820]

48. Jung Y-S, Qian Y, Chen X. Examination of the expanding pathways for the regulation of p21 expression and activity. Cellular Signalling. 2010; 22(7):1003–12. [PubMed: 20100570]

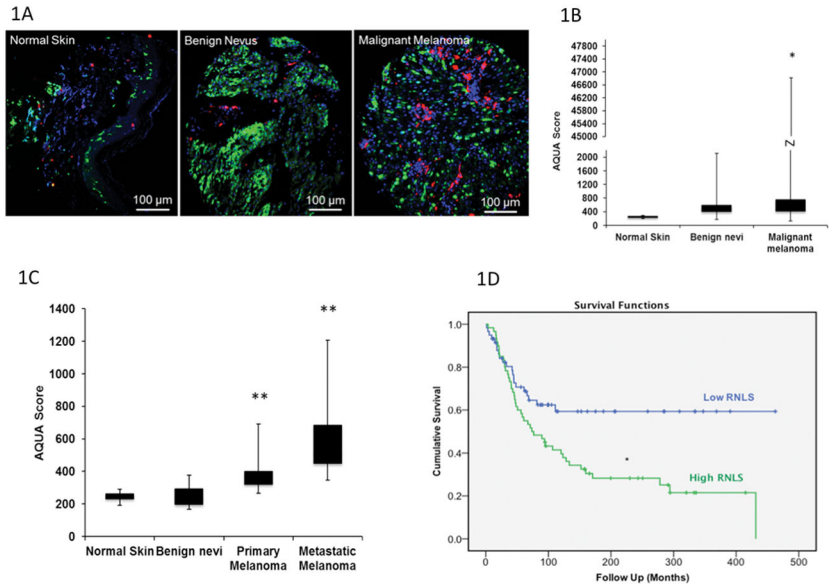

Figure 1. RNLS overexpression associated with poor outcome in melanoma

A: RNLS expression detected using m28-RNL, normal human skin (n=15), benign nevi (n=295), malignant melanoma (n=264); representative results, blue color: nuclei, green: melanocytes, red: RNLS.

B: Fluorescence intensity quantified by AQUAnalysis^{TM} software, Yale; TMA: normal human skin (n=15), benign nevi (n=295), malignant melanoma (n=264).

C: As in **B**; US Biomax TMA: human skin (n=14), benign nevi (n=14), primary melanoma (n=35), metastatic melanoma (n=11), *:p=0.009, **:p<0.001.

D: Kaplan-Meier survival curve, melanoma-specific death; 119 serial primary melanomas collected from 1997 to 2004, stratified into low and high RNLS expression using AQUA score=75,764.45, *:p=0.008.

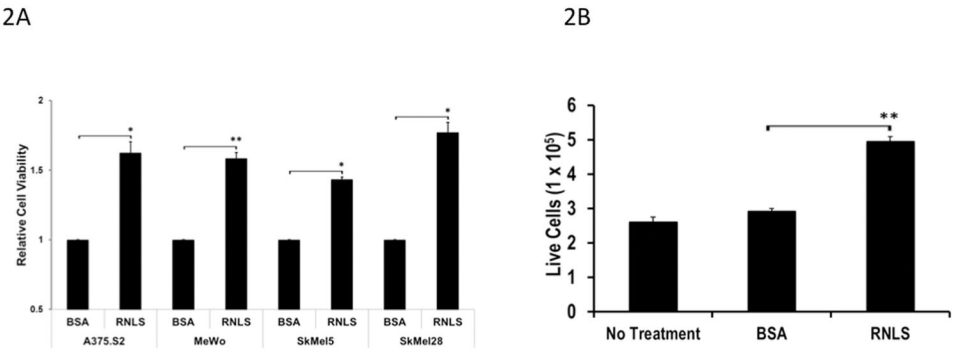

Figure 2. RNLS overexpression favors cancer cell survival

A: A375.S2, MeWo, Skmel5, Skmel28 cells serum-starved, treated with BSA (30 ug/ml) or rRNLS (30 ug/ml), cell viability at 72 hrs by WST-1; n=6, *:$p<0.05$, **:$p<0.005$.

B: A375.S2 cells serum-starved for 24 hrs, then untreated or incubated with 30ug/ml of BSA or rRNLS for 3 days; live cell number by trypan blue; n=6, **:$p<0.001$.

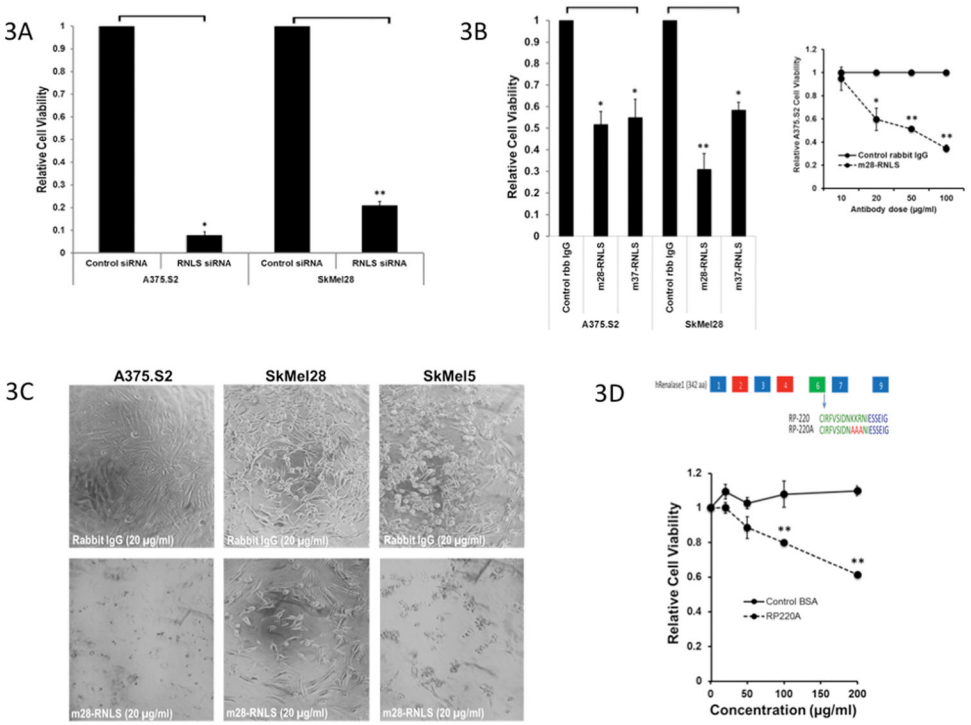

Figure 3. Inhibition of RNLS signaling is cytotoxic to melanoma cells

A: Transient transfection of A375.S2, SK-Mel-28 with RNLS-specific siRNA, or control siRNA, cell viability assessed 72hrs by WST-1; n=6, *:p=0.03, **:p=0.003.

B: *Left panel*: Cells treated with indicated antibodies for 72 hrs, cell viability by WST-1; m28-RNLS and m37-RNLS: RNLS monoclonals; *Right panel*: A375.S2 treated with m28-RNLS for 72 hrs,; n=6, *=p<0.05, **=p<0.005.

C: Representative photos A375.S2, SkMel28, SkMel5; 72 hrs incubation, rabbit IgG or m28-RNLS.

D: Amino acid (AA) sequence of RNLS peptide antagonist (RP220A). A375.S2 cells treated with as indicated, cell viability 72 hrs by WST-1; n=6, **=p<0.005.

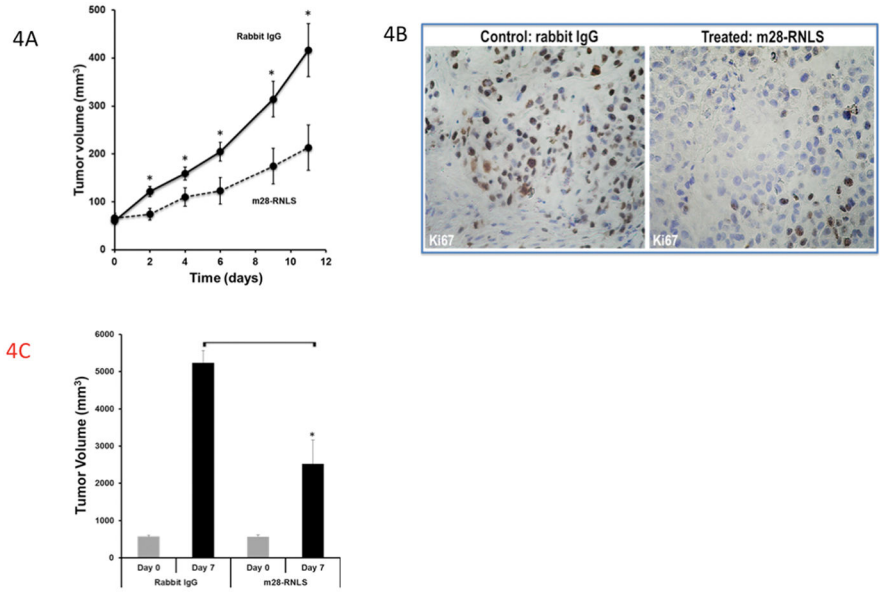

Figure 4. Inhibition of RNLS signaling blocks melanoma growth in vivo

A: Nude mice xenografted with A375.S2 cells, tumor size measured prior to treatment every 3 days with 2 mg/kg of rabbit IgG, or m28-RNLS; n=14 per group; *=p<0.05.

B: Representative IHC stains for Ki67 (brown color) in A375.S2 xenografted tumors (n=14 each) treated with m28-RNLS or rabbit IgG.

C. C57BL/6 mice xenografted with B16-F10 cells, treated every 3 days with 2 mg/kg rabbit IgG (n=5) or m28-RNLS (n=5); animals sacrificed day 7 due to large tumor burden in control group; *=p<0.025.

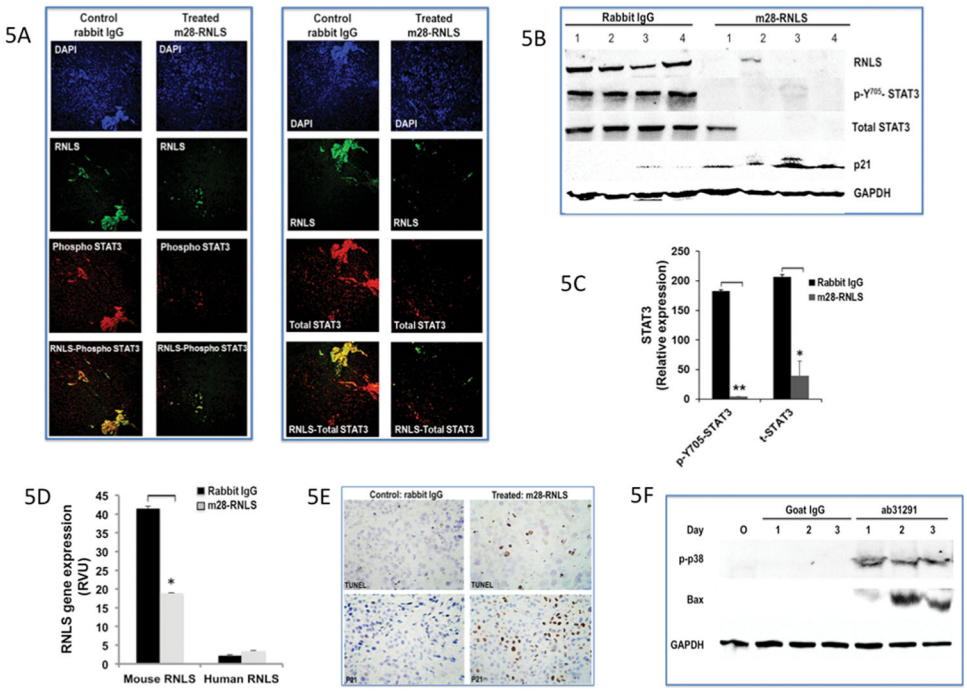

Figure 5. Inhibition of RNLS signaling blocks RNLS expression and STAT3 activation, induces apoptosis and cell cycle arrest

A: Xenografts treated with rabbit IgG or m28-RNLS, probed by immunofluorescence; phospho STAT3=p-Y^{705}-STAT3; representative results, blue color: nuclei, green: RNLS, and red: phospho STAT3 (left panel) or total STAT3 (right panel).

B: As in A, tumor cell lysates probed for RNLS, pSTAT3, totalSTAT3, p21 by western blot; representative results.

C: Quantification of STAT3 protein expression in samples shown in **B**; p-Y^{705}-STAT3 signals normalized to total STAT3, total STAT3 signals normalized to protein loading measurements; n=3, *:$p<0.05$, **=$p<0.005$.

D: Xenograft tumors (n=14 each) treated rabbit IgG or m28-RNLS, probed for human and mouse RNLS expression by qPCR, *=$p<0.05$.

E: IHC images of A375.S2 xenografted tumors (n=14 each) for TUNEL assay or p21 (brown color) treated with m28-RNLS or rabbit IgG.

F: A375.S2 cells treated with anti-RNLS antibody or goat IgG; time course of p38 phosphorylation and Bax expression by western blot; p-p38= phosphorylated p38; Bax=bcl-2 like protein 4.

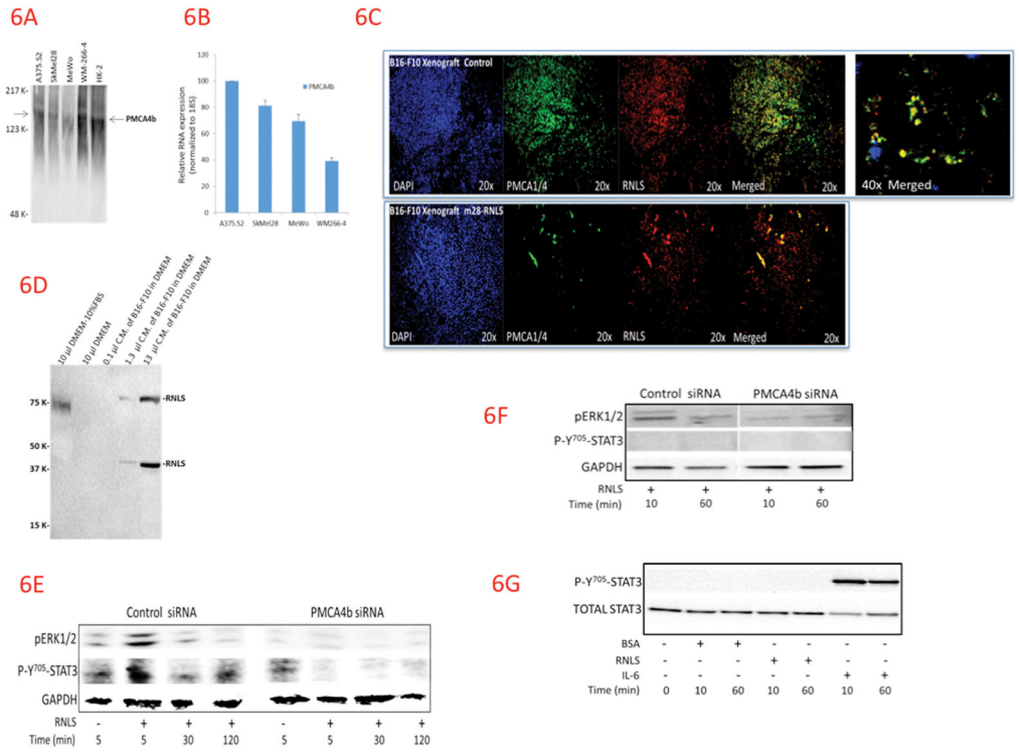

Figure 6. Extracellular RNLS signals via PMCA4b and phosphorylates ERK1/2 and STAT3 in B16-F10 melanoma cells

A: Lysates melanoma cell lines A375.S2, SkMel28, MeWo, WM266-4, and human kidney 2 positive control (HK-2) cells probed for PMCA4b by western blot; representative results, n=3.

B: Lysates melanoma cell lines A375.S2, SkMel28, MeWo, WM266-4 probed for PMCA4b by qPCR; mRNA levels normalized to 18S expression; n=3.

C: B16-F10 xenograft tumors treated with rabbit IgG (top panel) or m28-RNLS (bottom panel), probed for RNLS and PMCA4; blue color: nuclei, green: PMCA4, red: RNLS; representative result, n=5.

D: Samples of Dulbecco's Modified Eagle Medium (DMEM) with FBS, serum-free DMEM, and serum-free medium after incubation with B16-F10 cells for 72 hours were collected, probed for RNLS by western blot; FBS = fetal bovine serum; C.M. = conditioned medium; representative results.

E: B16-F10 cells transfected with control or PMCA4b siRNA, treated with BSA (30μg/ml) or rRNLS (30μg/ml) for indicated time, lysates probed by western blot; pERK1/2 = phosphorylated ERK; representative results; n=3.

F: Raw 267.4 blood macrophage cells transfected with control or PMCA4b siRNA, treated with rRNLS (30μg/ml) for indicated time, cell lysates probed as in E; representative study; n=3.

G: Mouse BMD macrophages treated with BSA (30μg/ml), rRNLS (30μg/ml) or interleukin 6 (IL-6) (50ηg/ml), cell lysates probed by western blot; P-Y^{705}-STAT3= phosphorylated STAT3 at tyrosine 705; representative study; n=3.

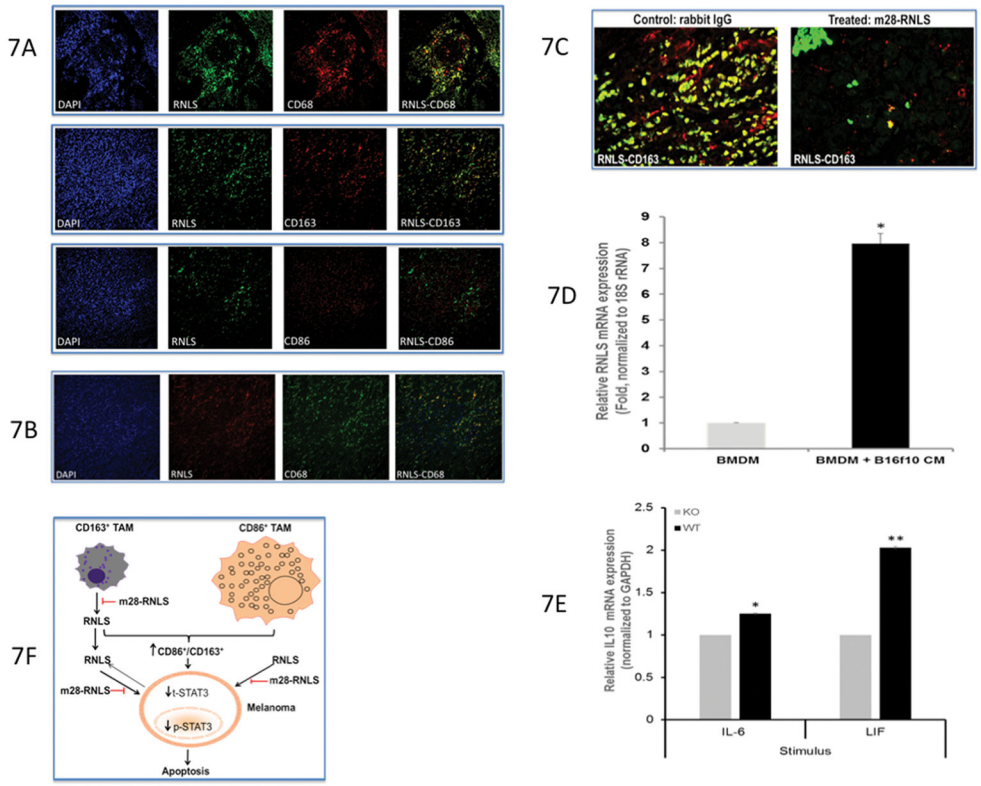

Figure 7. RNLS expressed in CD163+ TAMs in melanoma

A: *Top panel*: Human melanoma examined by IF for coexpression of RNLS and pan-macrophage marker CD68; blue color: nuclei, green: RNLS, and red: all macrophages; DAPI: nuclear stain, RNLS-CD68: merged RNLS and CD68 stains; *Middle panel:* Melanoma examined by IF for RNLS and M2 marker CD163; blue color: nuclei, green: RNLS, red: M2 macrophages; DAPI: nuclear stain, RNLS-CD163: merged RNLS, CD163 stains; *Lower panel:* IF of Melanoma for RNLS and M1 marker CD86; blue: nuclei, green: RNLS, red: M1 macrophages; DAPI: nuclear stain, RNLS-CD163: merged RNLS, CD86.

B: Xenograft in nude mice treated with rabbit IgG, probed for RNLS and macrophages (CD68+ cells) by immunofluorescence (n=4); representative results, blue: nuclei, green: macrophages, red: RNLS.

C: Xenograft treated with rabbit IgG or m28-RNLS, probed for RNLS and M2 TAMs (CD163+ cells) by immunofluorescence; representative result, green: M2 macrophages, red: RNLS.

D: Relative RNLS mRNA level by qPCR in BMD macrophages without or with conditioned medium from B16f10 (BMDM and BMDM + B16f10 CM, respectively), n = 4; *=$p<0.0001$.

E. Relative mRNA levels of IL-10 by qPCR in macrophages from WT (n=4) or RNLS KO mice (n=4) with indicated stimuli; * and **=$p<0.02$, 0.0001 respectively.

F: *Proposed mechanism of action of m28-RNLS.* Inhibition of RNLS signaling increases CD86+ to CD163+ TAMs ratio, decreases RNLS secretion from CD163+ TAMs, and inhibits RNLS signaling in melanoma, leading to significant reduction in total and phosphorylated STAT3 and apoptosis. TAM: tumor associated macrophages, CD163:

alternatively activated macrophage (M2) marker, CD86: classically activated macrophage (M1) marker, RNLS: renalase, m28-RNLS: antirenalase monoclonal antibody, t-STAT3: total STAT3, p-STAT3: phosphorylated STAT3.